

## Jumping via Robot Body Deformation - Mechanics and Mechanism for Higher Jumping

M. MIYAZAKI\* and S. HIRAI

*Dept. of Robotics, Ritsumeikan University,  
Kusatsu, Shiga 525-8577, Japan*

*\*E-mail: rr008035@se.ritsumei.ac.jp  
www.ritsumei.ac.jp/se/~hirai/*

As jumping is an effective method of moving over rough terrain, there is much interest in building robots that can jump. Deformation of a soft robot's body is an effective method to induce jumping. Our aim was to develop a jumping robot by deformation of a circular shell made of spring steel to result in the highest jump. Higher jumping requires enlargement of the contact area between the robot body and the floor. We developed a jumping mechanism that utilized a dish shape to maximize contact area.

*Keywords:* jumping, deformation, shape, mechanism

### 1. Introduction

Because jumping is a very effective method of maneuvering, especially over obstacles, jumping is used ubiquitously by animals and insects as a means of locomotion. For this reason, there are a variety of jumping robots, most of which have rigid bodies<sup>1-3</sup>. A flexible body exhibits high stability when moving in rough terrain. The aim of the present study is to improve the jumping capability of a soft robot.

### 2. Principle of Jumping via Robot Body Deformation

Figure 1 shows the principle of jumping. Deformation of the robot body results in the accumulation of energy. Instantaneous release of this energy causes the robot to jump. The principles of jumping include 1) bouncing off the ground (Fig. 1-(a)) and 2) stretching upward with a flat bottom (Fig. 1-(b)). A shape with a flat bottom has been reported have increased impulse during jumping, resulting in higher jumps<sup>4</sup>. We investigated which of the four initial deformation shapes, shown in Fig. 2, of a deformable robot that

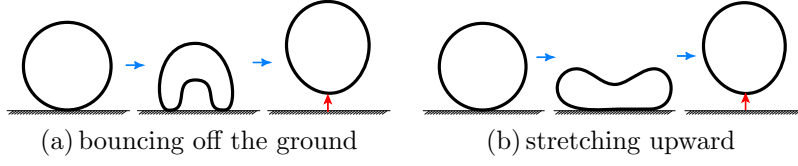


Fig. 1. Principle of jumping via deformation

is circular at rest results in the highest jump. The robot's body is made of spring steel, weighs 4.6 g, and is 100 mm in diameter, 12 mm in width, and 0.15 mm in thickness. All four shapes have the same flexural potential energy,  $U_{\text{flex}} = 16.0 \times 10^{-2} \text{ Nm}$ . Fig. 3 shows how each shape jumps. The arrows indicate the bottom of the objects in their highest positions and the value indicates the height of the bottom point. As shown in Fig. 3, the dish jumps the highest, followed in decreasing order by the peanut, cup, and cap. Clearly, jumping ability depends on the initial shape of deformation.

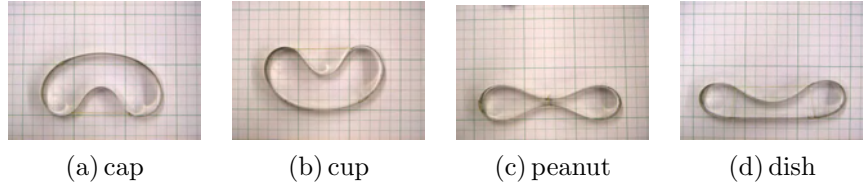


Fig. 2. Initial deformation shapes tested for jumping capability

### 3. Mechanics of Jumping

#### 3.1. Flexural potential energy

We next calculated the flexural potential energy of a circular body. If  $L$  is the length of the circumference,  $P(s)$  is a point on the body at distance  $s$  from the point of origin along the circumference, and  $\theta(s)$  is the angle subtended by the tangent to  $P(s)$ , the flexural potential energy of a circular robot can be calculated as:

$$U_{\text{flex}} = \int_0^L \frac{1}{2} R_{\text{flex}} \left( \frac{d\theta}{ds} \right)^2 ds, \quad (1)$$

where  $R_{\text{flex}}$  is the flexural rigidity at point  $P(s)$ . We used this equation to evaluate the flexural potential energy of a circular body during dynamic

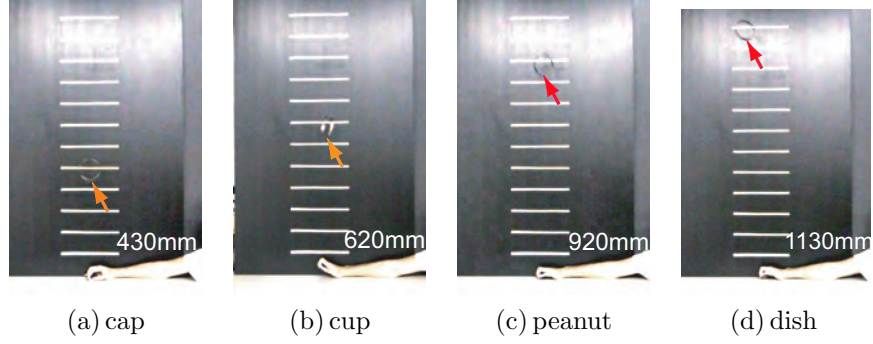


Fig. 3. Effect of initial deformation shapes on jumping

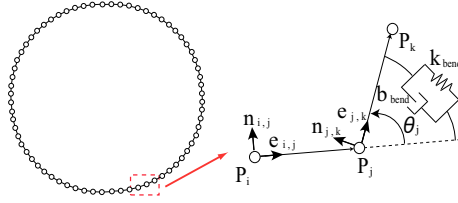


Fig. 4. Flexural Voigt model around a shell particle

simulation.

### 3.2. Particle-based model of circular robot

Figure 4 shows the flexural Voigt model around a shell particle.  $P_i$  and  $P_k$  are the particles adjacent to  $P_j$ , separated by angle  $\theta_j$  around particle  $P_j$ . The torque  $\tau_j$  around particle  $P_j$  is then given by

$$\tau_j = k_{\text{bend}}\theta_j + b_{\text{bend}}\dot{\theta}_j, \quad (2)$$

where  $k_{\text{bend}}$  is the flexural elastic constant,  $b_{\text{bend}}$  is the flexural viscous constant,  $e_{i,j}$  is the unit vector along the edge from  $P_i$  to  $P_j$  and  $n_{i,j}$  is the unit vector perpendicular to vector  $e_{i,j}$ . We assume that vectors  $e_{i,j}$  and  $n_{i,j}$  form a right-handed coordinate system. Distance  $l$  is fixed between two neighboring particles. Torque  $\tau_j$  can be equivalently converted into three forces,  $-(\tau_j/l)n_{i,j}$  on  $P_i$ ,  $-(\tau_j/l)n_{j,k}$  on  $P_k$  and  $(\tau_j/l)n_{i,j} + (\tau_j/l)n_{j,k}$  on  $P_j$ .

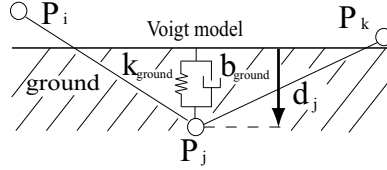


Fig. 5. Model of the ground

### 3.3. Model of the ground

Collision with the ground makes a circular robot jump. We therefore modeled the ground to simulate the collision between a robot and the ground. Fig. 5 shows a Voigt model of the ground, where  $k_{\text{ground}}$  is the coefficient of elasticity and  $b_{\text{ground}}$  is the coefficient of viscosity. Particle  $P_j$  is assumed to be beneath the surface of the ground, and  $d_j$  is the depth to which particle  $P_j$  has penetrated the ground. A repulsive force  $f_{\text{ground}}$  is then applied to the particle. This repulsive force can be expressed as:

$$f_{\text{ground}} = k_{\text{ground}}d_j + b_{\text{ground}}\dot{d}_j. \quad (3)$$

If  $\mu$  is the coefficient of friction of the ground, then, the force of friction on particle  $P_j$  is  $\mu f_{\text{ground}}$ .

### 3.4. Impulse from the ground during jumping

We next simulated the reaction force and the impulse from the ground during the jumping process. Fig. 6 shows the reaction force from the ground during jumping on the shapes shown in Fig. 2. Fig. 6-(d) shows reaction forces on the dish shapes in Fig. 2-(d). No impulsive force is generated. A relatively small force is applied for a longer time, almost 15 ms. The result indicates that the maximum reaction force from the ground does not directly influence the height of the jump. The impulses of the particles from the ground can be computed by integrating the force with respect to time. Fig. 7 shows the calculated results. When the stored flexural potential energy of the initial shapes is identical, the maximum reaction force of the dish is the lower than for the other three shapes. Surprisingly, the maximum impulse of the dish is optimal. Comparison of the Fig. 2, jump height is related to the maximum force of the impulse.

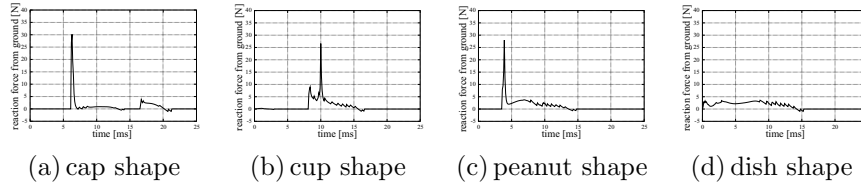


Fig. 6. Reaction force from the ground

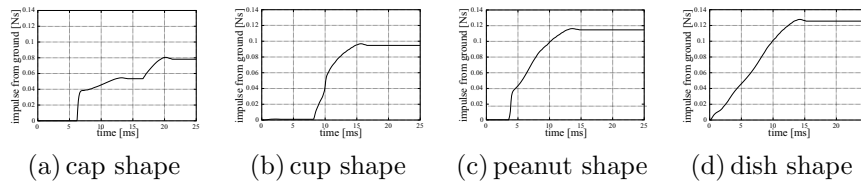


Fig. 7. Impulse from the ground during jumping

#### 4. Jumping Mechanism

##### 4.1. Realization of a dish shape

We developed a special mechanism to realize the dish shape, as shown in Fig. 8. The mechanism includes a frame and a wire (Fig. 8-(a)). By pulling the wire, the frame is pushed toward the robot body, making it flat (Fig. 8-(b)).

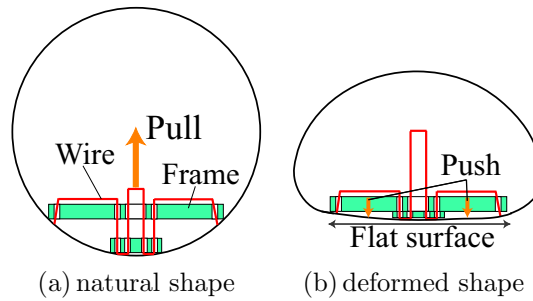


Fig. 8. Mechanism for the dish shape

#### 4.2. Wire pulling and releasing

The wire must be pulled to deform the robot body from its natural shape into the dish shape. By releasing the wire, the dish shape turns into the natural shape, making the robot jump. The wire should be released quickly for the robot to jump. We therefore used a quick return mechanism (Fig. 9) to pull and release the wire. The end of the wire is fixed to the rigid bar. When the rigid bar moves to the opposite side, the wire is wound around the curved body of the mechanism. This mechanism works repeatedly in order of Fig. 9-(a) to (d).

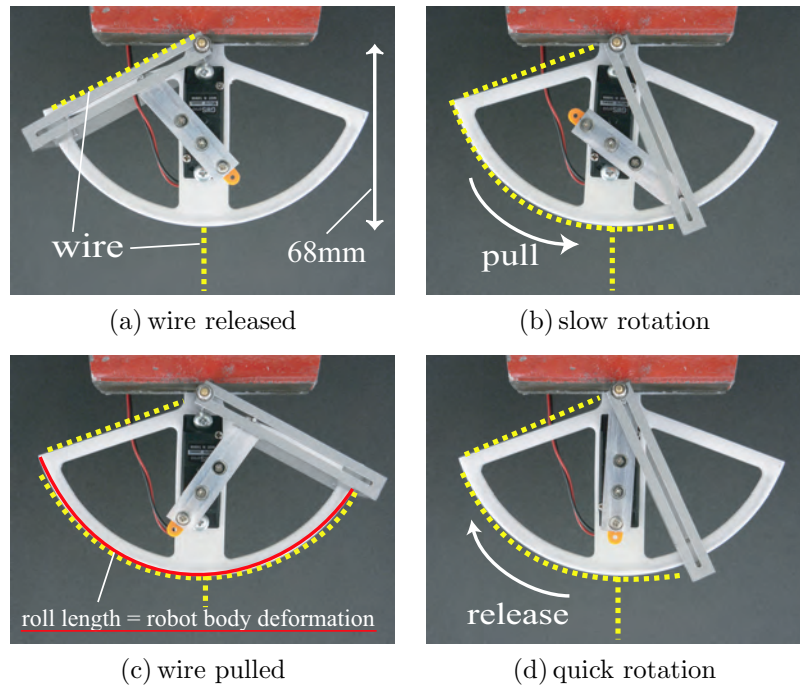


Fig. 9. Quick return mechanism

#### 4.3. Prototype

We made a prototype of a jumping robot (Fig. 10-(a)), using a dish shape mechanism weighing 10.7 g, a quick return mechanism weighing 51.6 g, and spring steels weighing 31.9 g, yielding a total robot weight of 94.2 g. The

spring steels were 200 mm in diameter, 15 mm in width, and 0.20 mm in thickness. By pulling the wire, the robot body was converted from its natural shape (Fig. 10-(b)) into the dish shape (Fig. 10-(c)). Jumping with the dish shape was achieved by this prototype. When the voltage of 6.0 V was applied to the robot, it could jump up to 35 mm in height (Fig. 11). In designing the wire pulling system, the robot body deformation was constrained to a maximum of 130 mm. However, because the motor torque is insufficient, the attainable deformation was only 115 mm. Because of this, the maximum jumping height of the robot was about 35 mm.

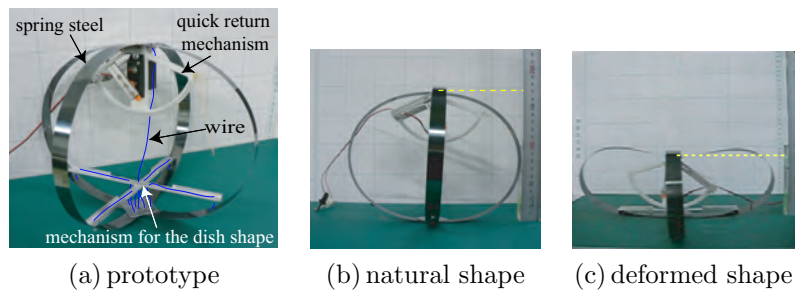


Fig. 10. Prototype of a jumping robot

## 5. Conclusion

We have demonstrated here the principle of jumping via robot body deformation. We found that, of the four initial shapes of deformation, the dish shape was able to jump the highest. The results of our simulation showed that impulse was important for jumping. An experimental prototype was constructed, its ability to attain a dish shape was evaluated, and its jumping performance was determined. Higher jumping requires increasing the motor torque by installing a gear in the motor and increasing the degree of deformation.

## References

1. H. Tsukagoshi, Y. Mori, M. Sasaki, T. Tanaka, and A. Kitagawa, Development of Jumping and Rolling Inspector to Improve the Debris Traverse Ability, *Journal of Robotics and Mechatronics*, Vol.15, No.5, pp.482-490, 2003.

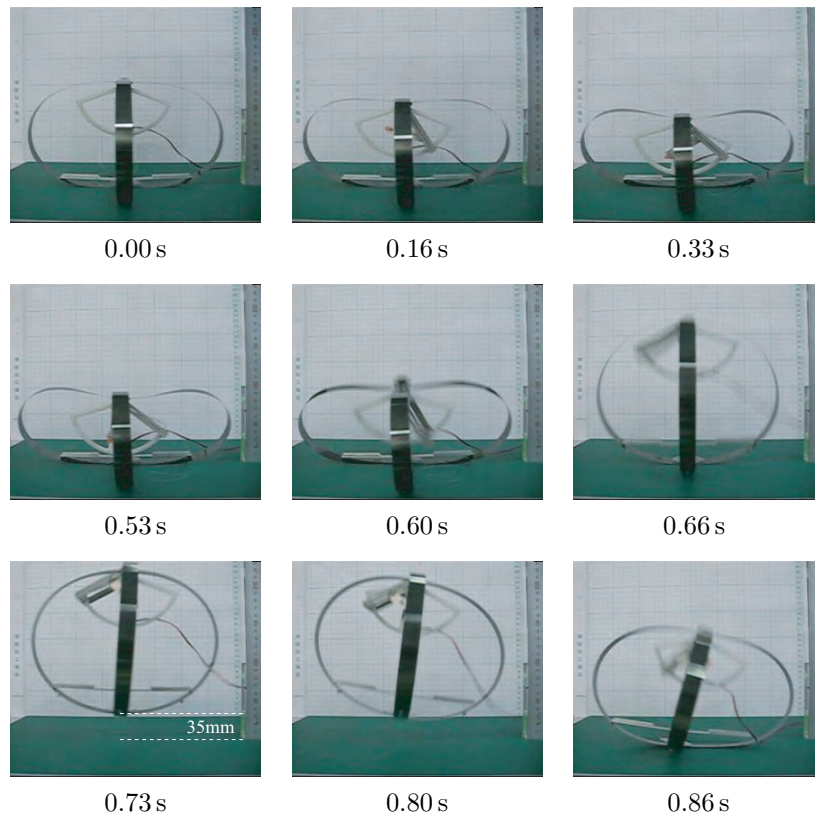


Fig. 11. Jump of a robot

2. S.B. Kesner, J.S. Plante, P.J. Boston, T. Fabian, and S. Dubowsky, Mobility and Power Feasibility of a Microbot Team System for Extraterrestrial Cave Exploration, *Proc. IEEE Int. Conf. on Robotics and Automation*, pp.4893-4898, Rome, April, 2007.
3. Y. Sugiyama, A. Shiotsu, M. Yamanaka, and S. Hirai, Circular/Spherical Robots for Crawling and Jumping, *Proc. IEEE Int. Conf. on Robotics and Automation*, pp.3595-3600, Barcelona, April, 2005.
4. Y. Matsuyama and S. Hirai, Analysis of Circular Robot Jumping by Body Deformation, *Proc. IEEE Int. Conf. on Robotics and Automation*, pp.1968-1973, Rome, April, 2007.